Lanthanide Triflates as Curing Initiators for Solid DGEBA Resin: Thermal and Mechanical Characterization

S. J. García,[1,2] A. Serra,[3] J. Suay[1]

[1]Centro de Biomateriales, Universitat Politècnica de València, Camino de Vera s/n, E-46071 Valencia, Spain
[2]Àrea de Ciencia de los Materiales, Departament d'Enginyeria de Sistemes Industrials i Disseny, Universitat Jaume I, Avda. Vicent Sos Baynat s/n, 12071 Castellón, Spain
[3]Departament de Q. Analítica i Q. Orgànica, Facultat de Química, Universitat Rovira i Virgili, C/Marcel·lí Domingo s/n. 43007 Tarragona, Spain

ABSTRACT: A new class of cationic initiators, lanthanide triflates, has been studied in the curing of diglycidyl ether of bisphenol-A (DGEBA). Two metal salts (Erbium and Ytterbium (III) trifluoromethanesulfonate) in various proportions (0.5, 1, and 2 parts per hundred of resin) have been used and the thermal and mechanical properties of the thermosets compared to a common solid epoxy system (crosslinked with *o*-tolylbiguanide). The kinetics of these processes has been evaluated by the isoconversional method that has been proved to be an excellent tool to predict the principal curing parameters (conversion/time/temperature). Their mechanical properties have been evaluated by dynamic mechanical thermal analysis (DMTA), stress-strain curves, impact resistances and adhesion to metallic substrates, and the thermal characteristics were measured by calorimetry (DSC) and thermogravimetry (TGA). © 2007 Wiley Periodicals, Inc. J Appl Polym Sci 105: 3097–3107, 2007

Key words: lanthanide triflate; cationic polymerization; thermal properties; mechanical properties; coatings

INTRODUCTION

Catalysts are important in polymerization processes because they decrease the activation energies and accelerate the reaction. They can be stimulated by heating or photoirradiation but, from the practical point of view, heating is the easiest option: homogeneous heating of reaction mixtures can be achieved without difficulty.[1] Moreover, elementary reactions are accelerated and the viscosity of the reaction mixture decreases in the first steps of the reaction.

Among the new thermal initiators, sulfonium, amonium, phosphonium, and hydrazinium salts are described as latent initiators that can polymerize epoxide monomers by a cationic mechanism. The order of reactivity of the cationic salts also depends on the nature of the counter anions: Cl^-, BF_4^-, SbF_6^-, PF_6^- being more active the less nucleophilic. Low nucleophilicity minimizes or prevents the reaction of the growing chain with the anion, which stops the growing of the polymeric chain.

It is well documented[2] that the high acid character and great oxophilicity of lanthanide compounds is highly improved in the case of lanthanide triflates because of the electron-withdrawing capacity of the anionic group. Lanthanide cations can coordinate to the epoxide oxygens leading to a weak C—O bond. The lanthanide trifluoromethane-sulfonate salts studied in this article contain an anion with an extremely poor nucleophilicity. Therefore, very low proportions of chain-end processes are expected.

The most widely used cationic polymerization catalyst in the field of epoxy technology has been the BF_3/amine compound. Epoxy formulations catalyzed by these compounds are relatively stable at room temperature and cure rapidly when exposed to high temperature. Unlike them, lanthanide triflates are stable even in aqueous media and have strong Lewis acid character. Lanthanide ions have low electronegativity and strong oxophilicity, which allows the metal to tightly coordinate to the oxiranic oxygen. They have large ionic radii and their coordination sphere can be modified leading to a different activity. All these characteristics allow the creation of template structures in the epoxide network.[3]

In the present work, we have studied the possibility to use two lanthanide triflates (erbium and ytterbium triflates) in the thermal crosslinking process of medium molecular weight diglycidyl ether of bisphenol-A resins as initiators and as catalysts of a conventional powder system epoxy/*o*-tolylbiguanide. Ytterbium

TABLE I
Composition of the Studied Samples

Sample	Epoxy resin	TBG (phr[a])	Benzoine (phr[a])	Flux Agent (phr[a])	Er(TfO)$_3$ (phr[a])	Yb(TfO)$_3$ (phr[a])
TBG	100	4.8	0.18	1.27	–	–
TBG/Er(TfO)$_3$ 1phr	100	4.8	0.18	1.27	1	–
TBG/Yb(TfO)$_3$ 1phr	100	4.8	0.18	1.27	–	1
Er(TfO)$_3$ 0.5phr	100	–	0.18	1.27	0.5	–
Er(TfO)$_3$ 1phr	100	–	0.18	1.27	1	–
Er(TfO)$_3$ 2phr	100	–	0.18	1.27	2	–
Yb(TfO)$_3$ 0.5phr	100	–	0.18	1.27	–	0.5
Yb(TfO)$_3$ 1phr	100	–	0.18	1.27	–	1
Yb(TfO)$_3$ 2phr	100	–	0.18	1.27	–	2

[a] phr, parts per hundred resin (w/w).

and erbium triflates were chosen among other lanthanide triflates because their coordinative abilities are similar and might not produce great variation in the reaction rate. The curing conditions, and the mechanical, morphological, and adhesion to metal properties of the cured materials have been obtained to test their potential use in powder coating industrial applications.

EXPERIMENTAL

Materials

Nine different samples (see Table I) were prepared using a solid bisphenol-A based epoxy resin of medium molecular weight (Scheme 1), and an average equivalent weight of 733 g/equiv ep. A first sample, used as the reference one, was the epoxy resin polymerized in the ratio given by the producer with a Huntsman *o*-tolylbiguanide (TBG), with an H$^+$ active equivalent weight of 37 g/equiv. The same system was catalyzed with two lanthanide triflates (erbium III and ytterbium III trifluoromethanesulfonate) in a proportion of 1 phr (parts of initiator per hundred of resin, w/w). Both triflates were also used to promote the homopolymerization of the same epoxy resin. To do so, three different proportions of each triflate were prepared: 0.5, 1, and 2 phr of each one.

Those materials, when applied on steel substrates for impact resistance tests, were formulated with benzoine (0.18 phr) to avoid porosity, and flux agent (1.27 phr) to allow the application by corona spray as powder coating.

Production of materials

Samples were premixed and hand-shacked until good dispersion was afforded. After that, the materials were extruded in a single screw extruder (Haake Rheomex 254), where operating conditions were 80°C along the extruder and 60 rpm. After extruding, the materials were grinded in an ultra-centrifugal mill ZM 100 and sieved at 100 micron, obtaining the different powder coatings ready to be applied on steel substrates or cured as free films for mechanical studies.

For the impact resistance tests the materials were applied on cold-rolled low-carbon steel normalized tests panels ($15 \times 7.5 \times 0.1$ cm^3). All test panels were degreased with acetone, and the powders were deposited by means of a corona electrostatic powder gun (powder coating equipment Easy 1-C). The epoxy formulations were totally cured for 15 min at 150°C in an oven (25 min for the samples using TBG, reaching total cure). Curing conditions were established after the kinetic study and with the objective of fixing a general curing condition. Thicknesses determined were always within the range 60 ± 5 μm.

For mechanical and thermal tests the materials were deposited manually on a polypropylene substrate and cured in an oven at 150°C for 1 hour assuring that the samples reach the total cure. After curing, the samples were peeled and tested.

Reactions taking place

Depending on the formulation used, different chemical reactions during curing process can take place giv-
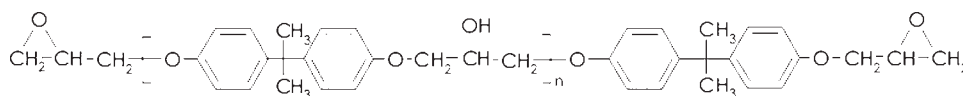
Scheme 1 DGEBA resin.
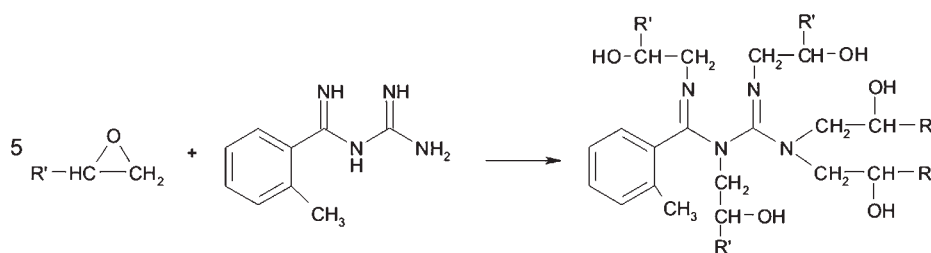
Scheme 2 Reaction O-tolylbiguanide (TBG) oxirane ring.

ing various networks with different structures and properties. Principal reactions are:

1. In epoxy systems using TBG the reactions taking place are between amino and oxirane groups[4] (Scheme 2).

   This kind of reaction (in the proportions used in this work) produces the total curing of the system in a range of temperature above 160°C. This polycondensation process produces shrinkage of the system during the curing, and as Scheme 2 shows a high number of hydroxylic groups are formed which can promote the adhesion to the metallic substrate.[5]

2. When adding to this system (epoxy-TBG) a lanthanide triflate as catalyst, the reaction presented in Scheme 2 becomes accelerated because of the creation of the oxiranic cation (Scheme 3), which promotes a faster reaction between the epoxy and the amine group of the TBG due to the high nucleophilicity of the nitrogen (higher than the one of the oxirane ring).[6]

3. In the case that we use lanthanide triflates to homopolymerize epoxy resins these compounds act as cationic ring-opening polymerization initiators and, therefore, two main mechanisms can be expected: the activated chain-end mechanism (ACE), which may be the most important one (Scheme 4), and the activated monomer mechanism (AM) as the secondary one (Scheme 5) which probably increases when more lanthanide triflate is added.[7,8] This kind of reactions also carries to a shrinkage which is usually lower than in case 1, because of the ring-opening polymerization mechanism. Moreover, these kind of reactions do not lead to the formation of hydroxyls, but lead to a highly crosslinked network and weakly plasticized (properties varying depending on the proportion of initiator used).[9]

Testing methods and equipment

Thermal characterization

A Perkin–Elmer DSC 7 differential scanning calorimeter was employed for dynamic scans to study the nonisothermal curing process and to apply the results to isothermal curing. The samples were analyzed in covered aluminum pans, using high purity indium sample for calibration. A flow of 20 cm³/min of argon was used as purge gas. The weight of the samples was between 8 and 9 mg. Nonisothermal scans were performed at rates of 2.5, 5, 10, and 15°C/min to not-cured-samples of the four prepared powder epoxy systems. The scans were done at the range of temperature from 25 to 300°C.

Isoconversional STARe software from Mettler-Toledo was used to calculate conversion degrees and kinetics of the process.

Differential scanning calorimeter was also used to determine the vitreous transition temperature (T_g) of the different cured samples. Scans were performed under the same conditions of the kinetic study using cured samples of 8 mg weight, at a scan rate of 10°C/min in the range of 25–250°C.

Thermogravimetric analysis (TGA)

To determine the influence of triflate salts on the thermal stability of an epoxy network thermogravimetric tests were carried out in a Setaram thermogravimetric analyzer (Setaram TGA92). Samples between 15 and 20 mg were scanned up to 900°C at 5°C/min. All scans were performed with an argon flow of 50 cm³/min.

Dynamic-mechanical thermal analysis (DMTA)

A dynamic mechanical Analyzer Seiko DMS210U was employed to perform mechanical measurements from 25 to 220°C at 1°C/min and a constant frequency of 1 Hz in three point bending mode.

From the theory of rubber elasticity[10,11] and using the modulus of relaxed material (E'_r) obtained from
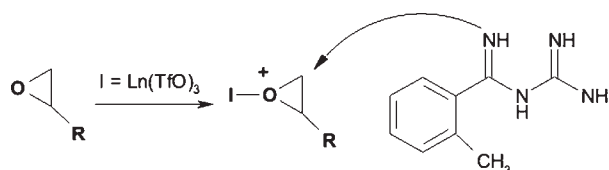
Scheme 3 Oxiranic cation produced by the presence of the triflate.
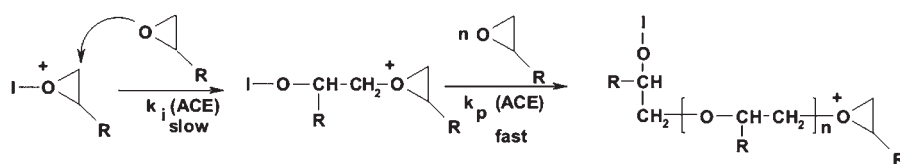
Scheme 4 Activated chain-end (ACE) mechanism.

the DMTA analysis (E' at $T_g + 50°C$), it can be calculated the average molecular weight between crosslinks ($\overline{M}_c$) by applying the simplified equation

$$\overline{M}_c = \frac{3\nu\rho RT}{E'} \tag{1}$$

where ν is the front factor ($\nu = 1$, in this work), ρ is the density of the sample, T is the temperature in Kelvin ($T = T_g + 50°C$) and R the universal gas constant.

The apparent density of the samples was calculated by an apparatus of density measurement (from Mettler-Toledo) coupled to a weight balance and using eq. (2).

$$\rho_{ap} = \frac{m_{air}}{m_{air} - m_{liq}}(\rho_0 - \rho_L) + \rho_L \tag{2}$$

where, ρ_0 is the density of the liquid (distilled water), ρ_L is the air density (0.0012 g/cm^3), m_{air} is the weight of the sample in air, and m_{liq} is the weight of the sample immersed in the liquid.

Morphology study—(scanning electron microscopy)

The morphology of the samples was studied with a scanning electron microscopy (SEM). Samples were frozen with liquid N$_2$ and hand broken. The measurements were carried out on a Jeol-JSM 6300 at 10 kV.

Mechanical tests (stress-strain curves)

Tensile testing up to failure was performed with an Adamel-Lomargy DY34 using a fixed crosshead rate of 10 mm/min with a 1 kN cell. Five cured samples of each formulation were standardly cut and tested so the results were an average of five tests. Traction tests were performed according to ASTM D 1708 96 and D 638. Young's modulus was calculated in the region of deformation over 0.5%.

Impact resistance test

Samples were deposited and cured on steel substrates. A 1-kg dart-mass was impacted at the back of each sample at different highs up to 1 m. The effect of the impact was visually evaluated and compared.

Adhesion test

Adhesion test was performed in accordance to ISO 4587 (1979). It consists on the deposition of the powder clearcoat between two rectangular and cleaned steel substrates, giving rise to a glued area of 13×25 mm^2 (Fig. 1). When the powder is deposited, the two rectangular substrates are fixed by means of two pincers and cured for 150°C 1 hour. After the curing process and three days of ambient exposure, the samples were tested with an Instron Universal Test Machine 4469 H 1907 at a traction speed of 1 mm/min. The data of tension and deformation were registered. With the break force (F) and the glued area, the shear stress is obtained (σ_{shear} (MPa) $= F/$area), giving the adhesion of the clearcoats to the substrates. Almost all the specimens showed an adhesive failure type. Five probes of each sample were prepared and tested.

RESULTS AND DISCUSSION

Thermal properties

Curing kinetics and T$_g$

It is known that initiators have a large influence on the processability, mechanical properties, adhesion, long-term stability, reactivity in different chemical/physical environments, and even in the total cost of the resulting crosslinking polymers. As has been mentioned above, Lewis acids induce cationic polymerizations leading to homopolymerization reactions.

Homopolymerization of epoxides by cationic mechanism has been recently kinetically studied in samples where DGEBA was dissolved in methanol and
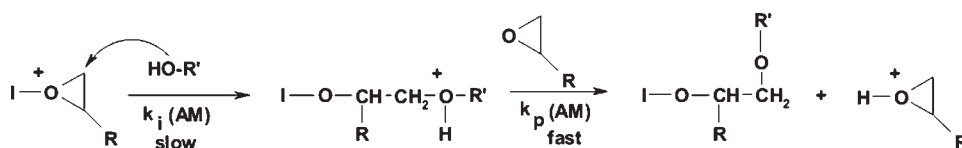
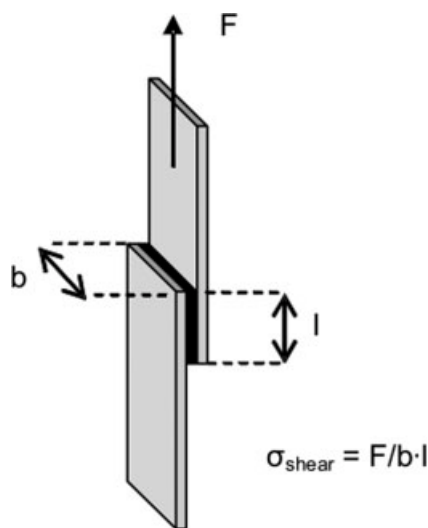**Scheme 5** Activated monomer (AM) mechanism.

Figure 1 Adhesion test.

the triflate salt in dichloromethane.[12] It has been established that propagation occurs via nucleophilic attack of the monomer and with the production of a polyether.

The physical and mechanical properties of a thermosetting resin mainly depend on the degree of cure. On the other hand, the processability of a thermoset depends on the rate and extent of polymerization under process conditions. Thus, the kinetic characterization of the reactive resin is not only important for a better understanding of structure–properties relationships, but also to optimize the processing conditions. Among a great number of experimental techniques relating to the research on thermosetting curing reactions, differential scanning calorimetry (DSC) has been used by a number of researchers to study the kinetics and thermal characteristics.

To study the curing kinetics of all the systems, four DSC scans were performed from 25 to 300°C at different heating rates for each formulation (2.5, 5, 10, and 15°C/min). With those scans and the use of the STARe software form Mettler-Toledo it can be

obtained the curing enthalpies (Table II), the activation energy and the conversion as a function of the temperature. Using the isoconversional method of the software, graphics of conversion in function of temperature and time can be plotted for systems formulated with erbium triflate (Fig. 2), and for systems formulated with ytterbium triflate (Fig. 3) both for a conversion of 90%. The representation of time against curing temperature for each system at a given conversion gives a comparative idea of the curing kinetics.

As it can clearly be seen for systems initiated by lanthanide triflates (homopolymerization), when more triflate is added the curing reaction is catalyzed and the curing rates are faster (as lanthanide triflate content increases the mechanism AM becomes more important and the curing is faster.) The curing enthalpies are almost the same independently on the proportion of triflate added, as expected. Moreover, the curing kinetics do not vary too much depending on the metal of the triflate (the coordinative abilities of the two lanthanide salts are similar and do not produce great variation in the reaction rate[9]) although systems with ytterbium present lower curing enthalpies values and slower curing rates.

When both lanthanide triflates are used in the presence of TBG there is a catalytic effect, although the curing rates are slower than for the cases where the lanthanide triflate is used to homopolymerize. The acceleration of the system using TBG, when triflate is added, is because of the activation of the epoxide ring as a cation by the metal. It could be expected that the first reaction should be the homopolymerization, nevertheless a complete kinetic study[6] showed that, due to the high nucleophilicity of TBG nitrogens, the reaction TBG/activated epoxide became accelerated and is the main process (Scheme 3), although the homopolymerization reactions could also take place but in a lower extent.

From the practical point of view, in the powder coating industry the curing time is normally in the range of 20–25 min, which means a curing temperature for a conventional system (using TBG) of 150°C

TABLE II
General Properties

Sample	ΔH (kJ/equiv ep)	T_g (°C)	$T_{degradation}$ (5% mass loss) (°C)	T_α(°C)	$T_\alpha +$ 50(°C)	E'_{rubber} (Pa)	ρ_{ap} (g/cm^3)	$\overline{M}_c$ (g/moL)
TBG	64.3	95	349	109	159	3.97E6	1.1048	2998.5
TBG/Er(TfO)$_3$ 1phr	62.5	100	337	110	160	4.59E6	1.1451	2690.9
TBG/Yb(TfO)$_3$ 1phr	66.6	97	337	108	158	4.08E6	1.1445	3010.9
Er(TfO)$_3$ 0.5phr	75.9	109	296	121	171	15.45E6	1.1437	819.2
Er(TfO)$_3$ 1phr	73.9	109	289	119	169	15.16E6	1.1305	821.5
Er(TfO)$_3$ 2phr	75.3	118	276	124	174	10.23E6	1.062	1156.3
Yb(TfO)$_3$ 0.5phr	62.8	107	299	119	169	15.22E6	1.1525	833.9
Yb(TfO)$_3$ 1phr	57.8	109	312	119	169	16.54E6	1.1469	763.8
Yb(TfO)$_3$ 2phr	68.7	115	277	123	173	8.87E6	1.1133	1396.0
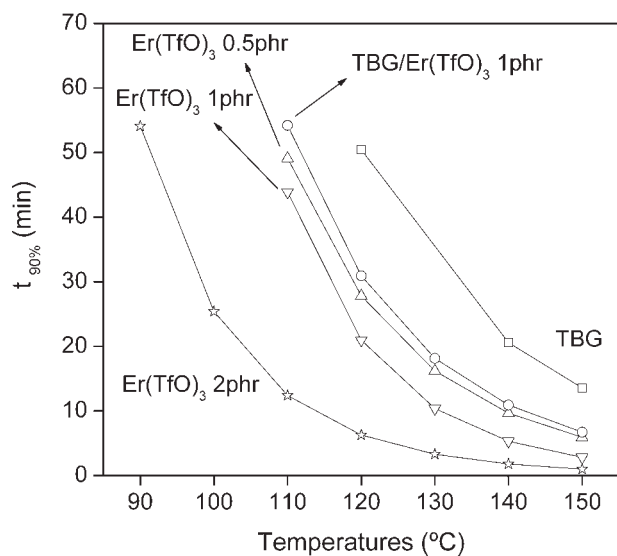
Figure 2 Time–Temperature for a 90% conversion of the systems with erbium triflate: epoxy resin/TBG (□), epoxy resin/TBG/erbium triflate 1 phr (○), epoxy resin/erbium triflate 0.5 phr (△), epoxy resin/erbium triflate 1 phr (▽), and epoxy resin/erbium triflate 2 phr (☆).

minimum while for a system using 2 phr of triflate the temperature can be reduced to nearly 100°C if additives are introduced for reducing the vitrifying effect (when curing temperatures are below the vitreous transition temperature, vitrification of the resin is produced). This fact can be a considerable advantage when using epoxy formulations as matrix of coatings especially if they have to be applied on thermosensible substrates (like wood or plastic).
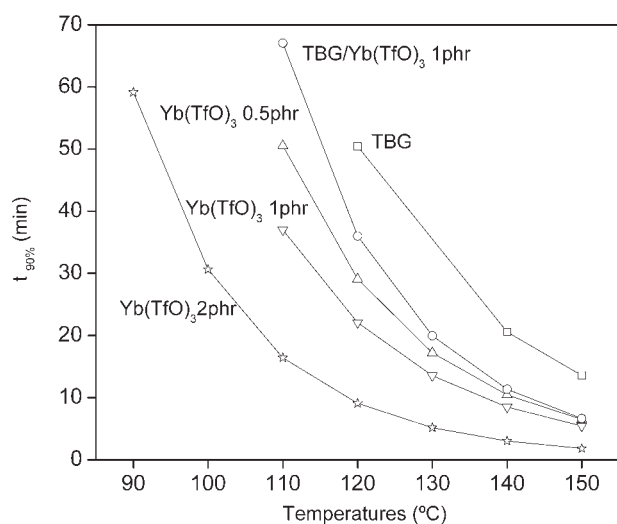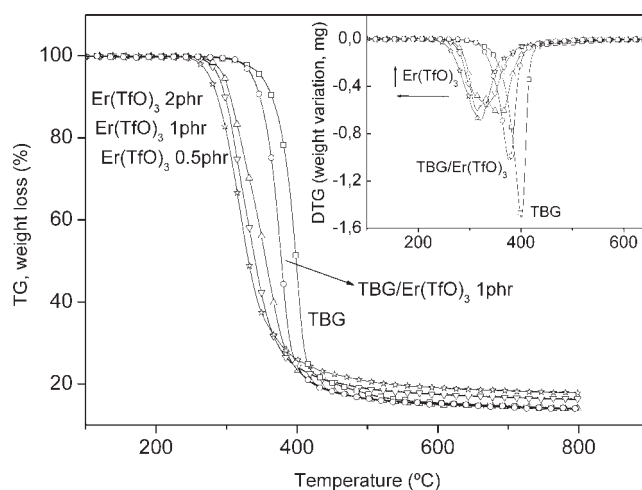
In Table II the different values of T_g can be seen. The use of lanthanide triflates increases the vitreous transition temperature in the homopolymerizing systems in a very similar way for erbium and ytterbium salts, being slightly higher when the proportion of initiator increases. The use of the lanthanide triflates as catalysts in systems epoxy-TBG slightly increases the T_g of the system. However, the values of T_g obtained in TBG systems do not reach the values obtained for homopolymerized thermosets.

Degradation process

Figures 4 and 5 shows the thermogravimetric curves of the thermosets obtained from systems formulated with erbium and ytterbium triflates, respectively. When the content of lanthanide triflate is increased there is a decrease in the thermal stability (thermal stability is always lower than that of the reference system).

A possible explanation to this fact can be found in the Lewis acid characteristics of the lanthanide triflates, which can help to break the ether linkages of the material by coordination of the metal to the ether group. The higher the content of lanthanide triflate the lower the initial degradation temperature (see Table II, data calculated at 5% of mass loss), which is due to the increase of the proportion of metals breaking the bonds. On the other hand, systems cured with TBG have higher thermal stability because of the lower number of ether groups and more unreactive groups coming from the attack of the TBG nitrogen to the epoxy ring (C—N bonds).

Figure 3 Time–Temperature for a 90% conversion of the systems with ytterbium triflate: epoxy resin/TBG (□), epoxy resin/TBG/ytterbium triflate 1 phr (○), epoxy resin/ytterbium triflate 0.5 phr (△), epoxy resin/ytterbium triflate 1 phr (▽), and epoxy resin/ytterbium triflate 2 phr (☆).

Figure 4 Thermogravimetric graphics obtained at 5°C/min for samples using Er(TfO)₃: epoxy resin/TBG (□), epoxy resin/TBG/erbium triflate 1 phr (○), epoxy resin/erbium triflate 0.5 phr (△), epoxy resin/erbium triflate 1 phr (▽), and epoxy resin/erbium triflate 2 phr (☆).
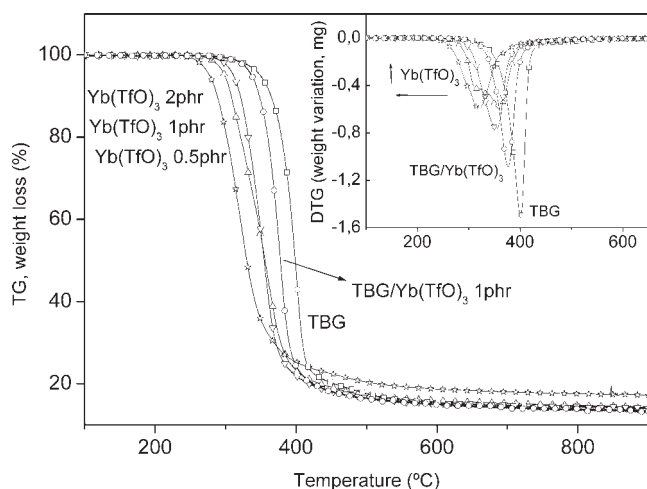
Figure 5 Thermogravimetric graphics obtained at 5°C/min for samples using Yb(TfO)$_3$: epoxy resin/TBG ($\square$), epoxy resin/TBG/ytterbium triflate 1 phr ($\bigcirc$), epoxy resin/ytterbium triflate 0.5 phr ($\triangle$), epoxy resin/ytterbium triflate 1 phr ($\triangledown$), and epoxy resin/ytterbium triflate 2 phr ($\star$).

Morphology study (SEM)

Figures 6 and 7 show the SEM-pictures at 75 magnifications of the thermosets obtained using erbium and ytterbium triflates, respectively. The lowest porosity is obtained for the samples cured with TBG (with or without lanthanide triflates). When the system is homopolymerized with lanthanide triflates there is an increase in porosity, being higher when more initiator is added. This increase of the macroporosity is probably due to the fact that the higher the curing rate the higher the increase of viscosity with time and the higher the probability of occluding air in the material. Sample with 2 phr of triflate has a special morphology. Not only it is full of macropores but also the resin particles are not sinterized at all, so the final structure is not homogeneous. The reason for this phenomenon can once more be the rapid curing kinetics for the 2 phr system that avoid the material to flow and to get sinterized.

DMTA

Dynamo-mechanical-thermal analysis of the cured samples were carried out to test the mechanical properties of these materials and to obtain more information of the extent of curing and morphology of the formed network. The results of the dynamic mechanical studies are presented in Figures 8 and 9. The principal drop in the storage modulus, and the corresponding maximum in the loss factor curve are because of the principal transition associated with the increase in internal freedom, such as long range segmental motions at the primary (α) transition.

The change of the mechanical relaxation as measured by the peak in the dynamic loss curve, and the change of the storage modulus, is often used to characterize the behavior of polymeric plasticizers and plasticized polymers.[13]

When lanthanide triflates are added to the epoxy system the peak of tanδ does not become broader, indicating no increase in the heterogeneity of the material. The peak also has a displacement towards higher temperatures as T_g does, indicating a possible
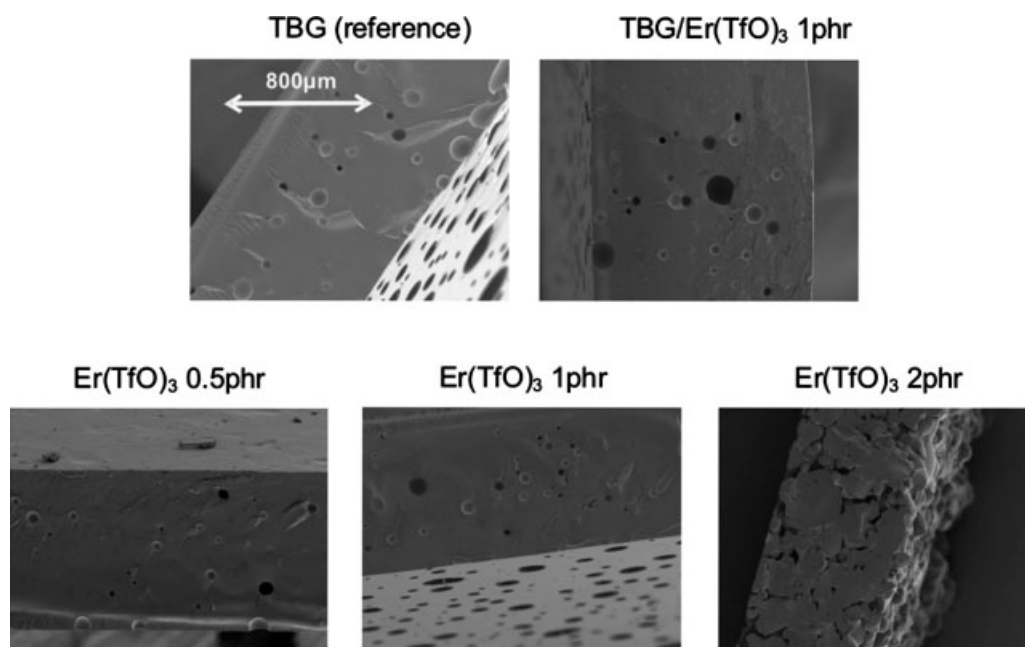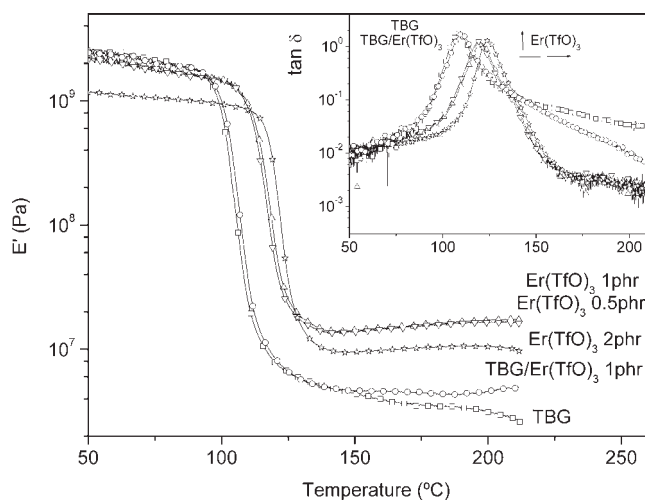

Figure 6 SEM pictures at 75 magnifications for samples using erbium triflate.

TBG (reference) TBG/Yb(TfO)$_3$ 1phr

Yb(TfO)$_3$ 0.5phr   Yb(TfO)$_3$ 1phr   Yb(TfO)$_3$ 2phr
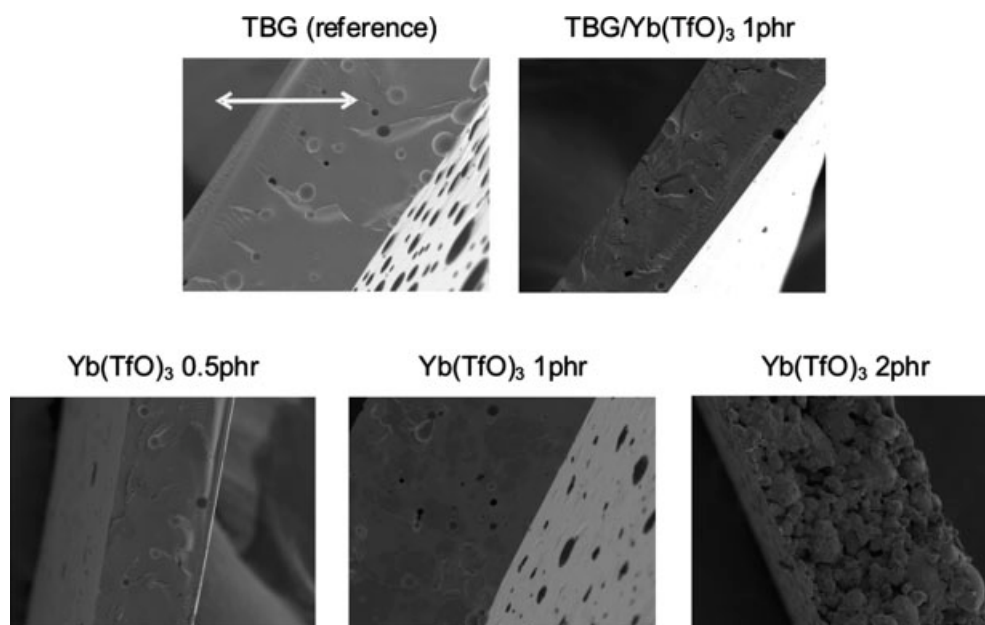
Figure 7 SEM pictures at 75 magnifications for samples using ytterbium triflate.

higher crosslinking density with lower mobility of the chains and less free volume in the network. Moreover the addition of lanthanide triflates increases the rubber storage modulus (E'_{rubber} in Table II) which implies that the material is more rigid and in accordance to the results obtained with tanδ, because of the increase of the crosslinking density. It should be said, that the network of the homopolymerized materials is much more compact than that one obtained from TBG as curing agent.

Molecular weight between crosslinks ($\overline{M}_c$)

Apparent densities (ρ_{ap}) and values of $\overline{M}_c$ are presented in Table II. It can be observed as was expected from other studies with lanthanide triflates[9] that the use of these compounds as initiators in the homopolymerization of epoxy resins leads to low molecular weight between crosslinks and a bigger crosslinking density as can also be observed from the T_g and T_α values. On the other hand, the reference system, obtained from catalyzed and un-catalyzed TBG,

Figure 8 Storage modulus (E') and loss tangent (tnδ) versus temperature obtained by DMTA for the formulations: epoxy resin/TBG (□), epoxy resin/TBG/erbium triflate 1 phr (○), epoxy resin/erbium triflate 0.5 phr (△), epoxy resin/erbium triflate 1 phr (▽), and epoxy resin/erbium triflate 2 phr (☆).
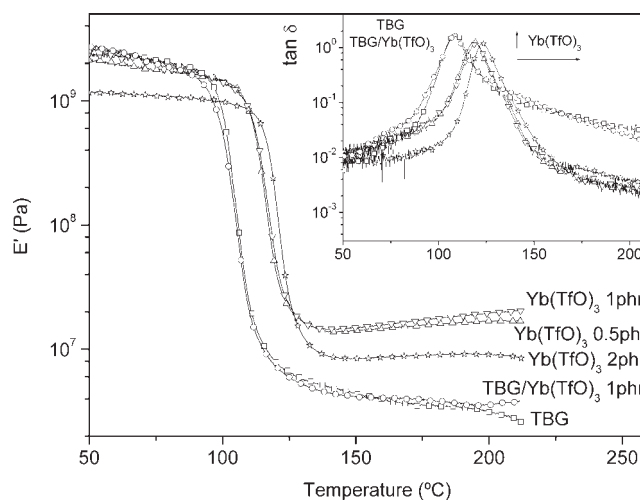
Figure 9 Storage modulus (E') and loss tangent (tnδ) versus temperature obtained by DMTA for the formulations: epoxy resin/TBG (□), epoxy resin/TBG/ytterbium triflate 1 phr (○), epoxy resin/ytterbium triflate 0.5 phr (△), epoxy resin/ytterbium triflate 1 phr (▽), and epoxy resin/ytterbium triflate 2 phr (☆).
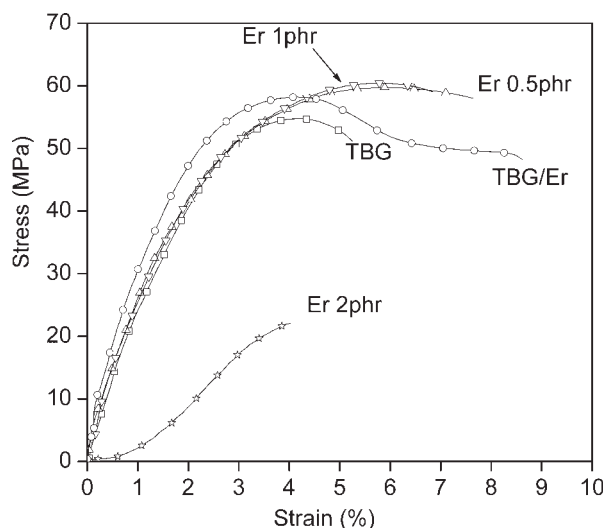
Figure 10 Stress-strain curves of the samples using erbium triflate: epoxy resin/TBG (□), epoxy resin/TBG/erbium triflate 1 phr (○), epoxy resin/erbium triflate 0.5 phr (△), epoxy resin/erbium triflate 1 phr (▽), and epoxy resin/erbium triflate 2 phr (☆).

presents much more $\overline{M}_c$ values than the samples homopolymerized with lanthanide triflates. This is due to the inclusion of the structure of the TBG in the network, which raises the value of $\overline{M}_c$.

Nevertheless samples with 2 phr of triflate present higher values of $\overline{M}_c$ and lower values of E′$_{rubber}$. This surprisingly result could be a consequence of the special morphologies of this type of materials, which are heterogeneous and full of macroscopic pores.

Stress-strain

Figures 10 and 11 show the stress-strain curves corresponding to the traction tests performed to the formulated coatings using erbium triflate and ytterbium triflate, respectively. Table III shows the parameters obtained from the mechanical tests: elastic modulus (E), elastic limit stress (σ_{el}), elastic limit strain (ε_{el}), maximum stress (σ_{max}), break stress (σ_{break}), break strain (ε_{break}), and toughness.

On comparing a homopolymerized system initiated by 0.5 or 1 phr of erbium triflate to a system having TBG, it can be observed that the homopolymerized materials present higher break deformation and stress (which implies higher ductility), higher toughness (which implies that homopolymerized samples can absorb more energy before they break down), and a slight increase of the elastic modulus (rigidity) that can be correlated to an increase in the crosslinking density (lower $\overline{M}_c$). The increase in rigidity can also be detected in the increase of T_g and T_α.

For samples initiated by ytterbium triflates results are less clear and effects less positive compared to systems with erbium salt. Proportions of erbium and

ytterbium salts of 2 phr showed no linear correlation with the lower proportions and they presented lower mechanical properties probably due to the lower sintering. When lanthanide triflates are used as catalysts in systems with TBG, there is also an increase of rigidity (higher E), increase of ductility (higher break strain), and higher toughness (more energy absorption before break).

Impact resistance

Figure 12 shows the pictures of the nine impacted samples at a height of 100 cm with a mass of 1 kg. For homopolymerized systems, a formulation with 1 phr of ytterbium triflate presents good impact resistance, while the other formulations with triflates did not. In any case, samples with ytterbium presented better results than those with erbium.

When the lanthanide triflates were employed as catalysts of a system with TBG, impact results were very good independently of the lanthanide triflate used.

A possible explanation of the good impact properties of samples with TBG and the bad ones in the homopolymerized systems can be the more expanded structure of the network when using TBG, and the higher internal stresses produced by the fastest curing of homopolymerized materials.[6–8,14]

Adhesion

Figure 13 shows the shear stress for the materials obtained using erbium and ytterbium triflates. A similar trend can be observed using both erbium and yt-
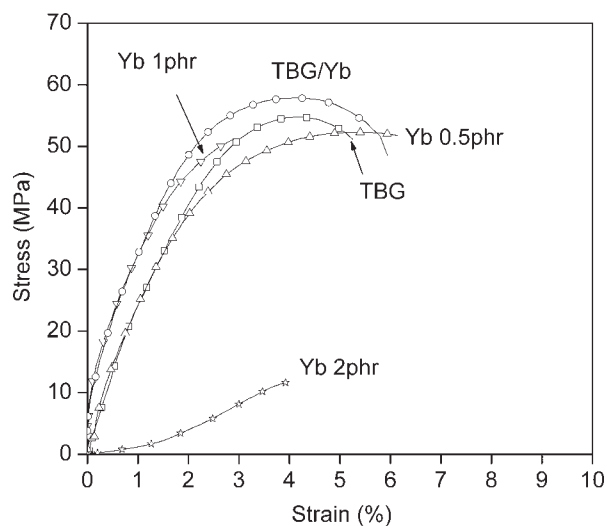
Figure 11 Stress-strain curves of the samples using ytterbium triflate: epoxy resin/TBG (□), epoxy resin/TBG/ytterbium triflate 1 phr (○), epoxy resin/ytterbium triflate 0.5 phr (△), epoxy resin/ytterbium triflate 1 phr (▽), and epoxy resin/ytterbium triflate 2 phr (☆).

TABLE III
Mechanical Properties from Stress–Strain Tests

Sample	E(MPa)	σ_{el} (MPa)	ε_{el} (%)	σ_{max} (kN)	σ_{break} (MPa)	ε_{break} (%)	Toughness (MPa)
TBG	1881.3 ± 205.6	46.7 ± 1.49	2.36 ± 0.13	56.01 ± 1.07	49.4 ± 0.77	5.55 ± 0.28	2.32 ± 0.114
TBG/Er(TfO)₃1phr	2479.9 ± 363.2	46.7 ± 1.01	2.107 ± 0.26	55.20 ± 2.79	46.26 ± 2.34	7.75 ± 0.84	2.82 ± 0.51
TBG/Yb(TfO)₃ 1phr	2410.4 ± 223.7	45.2 ± 2.81	2.08 ± 0.14	59.63 ± 0.40	49.65 ± 3.27	6.85 ± 1.29	3.23 ± 0.062
Er(TfO)₃ 0.5phr	2328.1 ± 217.7	46.1 ± 2.82	2.40 ± 0.20	59.21 ± 0.54	57.50 ± 0.56	6.97 ± 1.26	3.35 ± 0.72
Er(TfO)₃ 1phr	1894.8 ± 139.0	52.12 ± 1.56	2.96 ± 0.12	59.05 ± 2.33	57.62 ± 1.45	6.66 ± 0.94	3.18 ± 0.63
Er(TfO)₃ 2phr	No linear behavior			21.88 ± 1.17	21.88 ± 1.17	4.04 ± 0.43	0.38 ± 0.061
Yb(TfO)₃ 0.5phr	1901.6 ± 234.6	49.56 ± 2.39	3.35 ± 0.62	53.94 ± 1.65	53.40 ± 1.50	5.92 ± 0.37	2.50 ± 0.24
Yb(TfO)₃ 1phr	2464.9 ± 123.9	44.35 ± 3.46	2.01 ± 0.23	48.37 ± 2.88	48.37 ± 2.88	2.49 ± 0.37	0.73 ± 0.22
Yb(TfO)₃ 2phr	No linear behavior			11.11 ± 0.54	11.11 ± 0.54	3.78 ± 0.16	0.16 ± 0.016

terbium triflates. The system with TBG presents the best adhesion to the substrate (high σ_{shear}), probably due to the hydroxyl groups produced in the reaction. A higher proportion of hydroxylic groups promotes a higher adhesion[15–18] to the metallic substrate because of the increase in the possibility to establish hydrogen bonds between both materials. It can also be seen that the use of lanthanide triflates lowers the dry adhesion to the steel substrate, being the higher the decrease when the higher the triflate content is. This trend is probably due to the inexistence of hydroxylic groups, the less polar character of the network, and the stress generated by the fast curing rate, and by a possible shrinkage which can lead to warping. Both ytterbium and erbium triflates showed similar results.

When lanthanide triflates were added as catalysts to TBG formulations there was also observed a decrease in adherence.
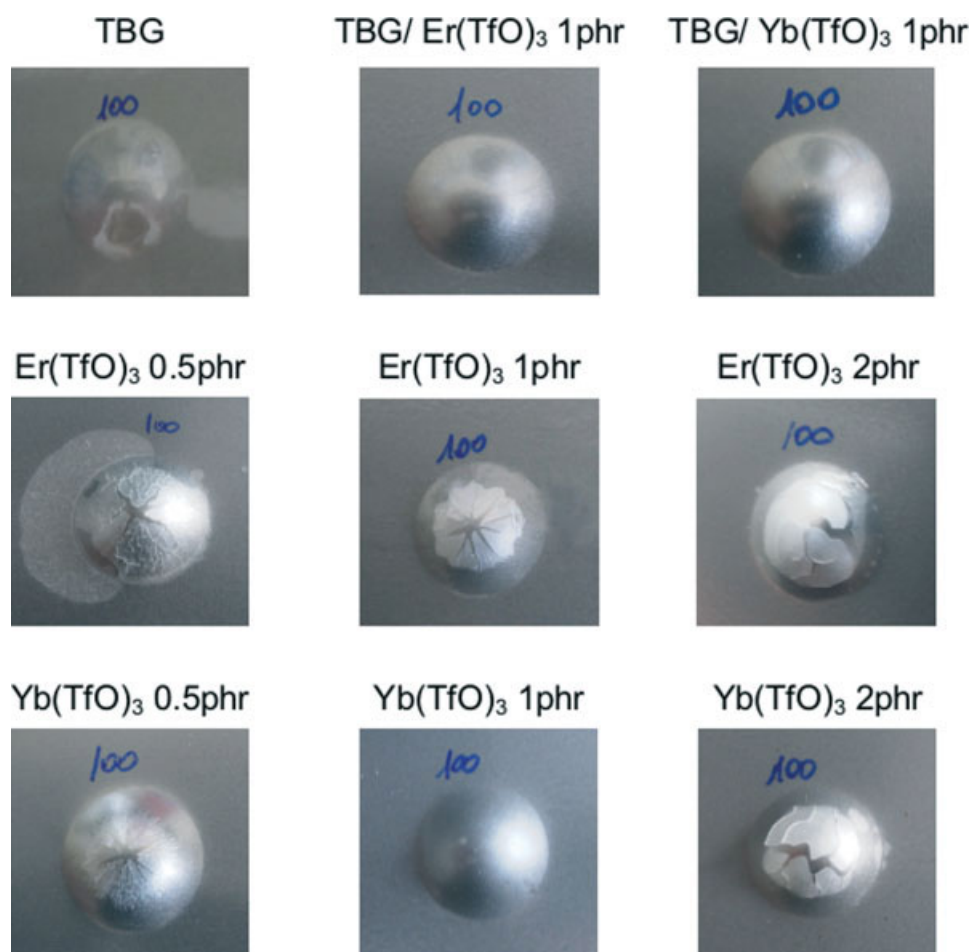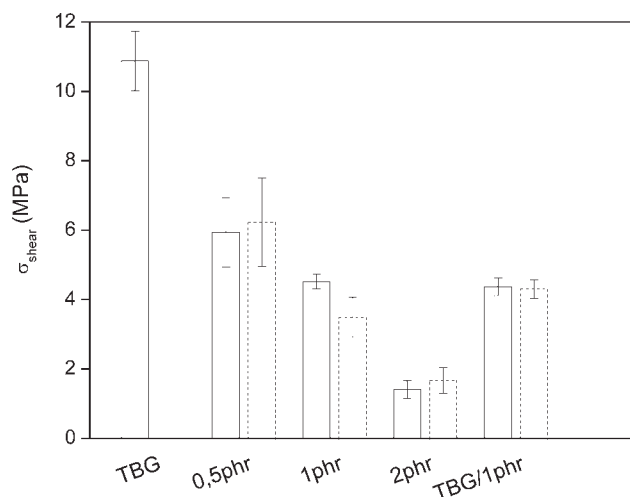

Figure 12 Impact resistance pictures of the prepared samples tested at 100 cm height with 1 kg of mass dart.

Figure 13 Shear stress of the samples formulated with: ytterbium triflate: solid line (—); and erbium triflate: dash line (- -).

CONCLUSIONS

The results obtained show that the use of erbium and ytterbium triflates as initiators of the homopolymerization of DGEBA resins, and as catalysts of systems epoxy/*o*-tolylbiguanide (TBG) diminishes the curing temperature and time with respect to the reference system DGEBA/TBG.

All samples using lanthanide triflates presented lower thermal stability compared to the reference system, being lower when a higher proportion of lanthanide triflate was added.

With respect to the influence on mechanical properties (including adhesion) and impact resistance, the homopolymerization of the epoxy resin by means of lanthanide triflates lead to good results when the proportion of lanthanide triflates was below 2 phr. Nevertheless, the systems did not offer mechanical properties as good as the system using TBG, probably due to the final composition of the epoxy network itself (nonexistence of OH^- groups in homopolymerized systems) and to the increase of internal stresses in the homopolymerized due to the fast curing rate.

The system with 1 phr of ytterbium salt (with and without TBG) presented a good combination of properties: good mechanical properties together with high curing rate.

As these new systems have proved to increase some important properties needed in powder coatings (such as reducing curing rate and fragility decrease) they can be an alternative to actual systems, although further research has to be done to improve mechanical and impact resistance properties.

References

1. Endo, T.; Sanda; F. Macromol Symp 1996, 107, 237.
2. Kobayashi, S. Synlett 1994, 689.
3. Aspinall, H. C.; Dwyer, J. L. M.; Greeves, N.; McIver, E. G.; Woolley, J. C. Organometallics 1998, 17, 1884.
4. Ochi, M.; Mimura, K.; Motobe, H. J Adhesion Sci Technol 1994, 8, 223.
5. Martí-Martínez, J. M.; Madrid-Vega, M. In Teoría de la adhesión, Tema 2: Propiedades de los adhesivos y los selladores antes del curado: Loctite Espa~na.
6. García, S. J.; Serra, A.; Ramis, X.; Suay, J. J. Therm Anal Calorim 2006. (August 2006 Online-first).
7. García, S. J.; Ramis, X.; Serra, A.; Suay, J. Thermochim Acta 2006, 441, 45.
8. García, S. J.; Ramis, X.; Serra, A.; Suay, J. Therm Anal Calorim 2006, 83, 429.
9. Mas, C.; Serra, A.; Mantecón, A.; Salla, J. M.; Ramis, X. Macromol Chem Phys 2001, 202, 2554.
10. Ramis, X.; Cadenato, A.; Morancho, J. M.; Salla, J. M. Polymer 2003, 44, 2067.
11. Tobolsky, A. V.; Carlson, D. W.; Indictor, N. J Polym Sci 1960, 54, 175.
12. Castella, P.; Galià, M.; Serra, A.; Salla, J. M.; Ramis, X. Polymer 2000, 41, 8465.
13. Rodríguez, M. T.; García, S. J.; Cabello, R.; Gracenea, J. J.; Suay, J. J. J Coat Technol 2005, 2, 557.
14. Mas, C.; Ramis, X.; Salla, J. M.; Mantecón, A.; Serra, A. J Polym Sci Part A: Polym Chem 2003, 41, 2794.
15. Greenfield, D.; Scantleburry, J. D. JCSE 2000, 3, paper 5.
16. Vaca-Cortés, E.; Lorenzo, M. A.; Jirsa, J. O.; Wheat, H. G.; Carrasquillo, R. L. In Adhesion Testing of Epoxy Coating; Centre for Transportation Research, Bureau of Engineering Research, University of Texas, Austin, 1998.
17. Gaynes, N. I. In Testing of Organic Coatings; Noyes Data: Park Ridge, NJ, 1977.
18. Lorenzo, M. A. Experimental Methods for Evaluating Epoxy Coating Adhesion to Steel Reinforcement. M.S. Thesis, University of Texas at Austin, 1997.